



LAWRENCE  
LIVERMORE  
NATIONAL  
LABORATORY

# Accuracy of Reduced and Extended Thin-Wire Kernels

G. J. Burke

November 25, 2008

The 25th International Review of Progress in Applied  
Computational Electromagnetics (ACES 2009)  
Monterey, CA, United States  
March 8, 2009 through March 12, 2009

## **Disclaimer**

---

This document was prepared as an account of work sponsored by an agency of the United States government. Neither the United States government nor Lawrence Livermore National Security, LLC, nor any of their employees makes any warranty, expressed or implied, or assumes any legal liability or responsibility for the accuracy, completeness, or usefulness of any information, apparatus, product, or process disclosed, or represents that its use would not infringe privately owned rights. Reference herein to any specific commercial product, process, or service by trade name, trademark, manufacturer, or otherwise does not necessarily constitute or imply its endorsement, recommendation, or favoring by the United States government or Lawrence Livermore National Security, LLC. The views and opinions of authors expressed herein do not necessarily state or reflect those of the United States government or Lawrence Livermore National Security, LLC, and shall not be used for advertising or product endorsement purposes.

# Accuracy of Reduced and Extended Thin-Wire Kernels \*

Gerald J. Burke

Lawrence Livermore National Lab., L-154, 7000 East Ave., Livermore, CA 94550  
burke2@llnl.gov, gjburke@ieee.org

**Abstract:** Some results are presented comparing the accuracy of the reduced thin-wire kernel and an extended kernel with exact integration of the  $1/R$  term of the Green's function and results are shown for simple wire structures.

The form for the thin-wire kernel in moment method codes has received considerable attention over the years. Early codes used a reduced kernel, with the evaluation points on the wire axis and the current represented as a filament on the surface. More recently the exact kernel has become popular, with the evaluation points on the wire surface and an accurate integration of the current over the cylindrical surface [1, 2, 3]. The exact kernel formulations have the advantage that wire segments can have arbitrarily small length relative to their radius. A widely used compromise has been to put the evaluation points on the surface and integrate the leading  $1/R$  term of the Green's function over the surface while using a filament approximation for the current with the more slowly varying remainder of the Green's function [4]. The accuracy of the latter form and the reduced kernel are compared here and some results for typical wire structures shown.

A typical integral to be evaluated for potentials at cylindrical coordinates  $\rho, z$  due to constant source density on a wire segment with length  $\Delta$  and radius  $a$  centered at the origin on the  $z$  axis is

$$K(\rho, z) = \int_{-\Delta/2}^{\Delta/2} \int_{-\pi}^{\pi} \frac{e^{-jkR}}{R} d\phi dz' \quad (1)$$

where  $R = \sqrt{\rho^2 + a^2 + (z - z')^2 - 2a\rho \cos \phi}$ . The inner integral over  $\phi$  in (1) is called the exact kernel. In [4], the  $1/R$  term is removed from a series expansion of the exponential in (1) and integrated accurately, while the reduced kernel approximation is applied to the remainder. This form, which will be called an extended thin-wire approximation (ETWK), is

$$K_1(\rho, z) = 2\pi \int_{-\Delta/2}^{\Delta/2} \frac{e^{-jkR_0} - 1}{R_0} dz' + \int_{-\Delta/2}^{\Delta/2} \int_{-\pi}^{\pi} \frac{1}{R} d\phi dz' \quad (2)$$

where  $R_0 = \sqrt{\rho^2 + a^2 + (z - z')^2}$  is  $R$  evaluated for  $\phi = \pi/2$ . The reduced kernel evaluation (RTWK) involves the single integral

$$K_0(\rho, z) = 2\pi \int_{-\Delta/2}^{\Delta/2} \frac{e^{-jkR_0}}{R_0} dz'. \quad (3)$$

The evaluation of integrals for the ETWK is much easier than with the exact kernel. The first integral in (2) is well behaved, and easily evaluated numerically. In the second integral the integration over  $\phi$  is sometimes done first to yield an elliptic integral of the first kind. This result must then be numerically integrated over  $z'$ , and if the evaluation point is on the segment it involves a singularity that may require extraction of an approximation of the

---

\* This work performed under the auspices of the U. S. Department of Energy by the Lawrence Livermore National Laboratory under Contract DE-AC52-07NA27344.

elliptic integral. An easier way may be to integrate over  $z'$  first to obtain

$$K_z(\rho, z, \phi) = \int_{-\Delta/2}^{\Delta/2} \frac{1}{R} dz' = \pm \log \left( \frac{z_2 \pm \sqrt{a^2 + z_2^2 + \rho_0^2 - 2a\rho_0 \cos \phi}}{z_1 \pm \sqrt{a^2 + z_1^2 + \rho_0^2 - 2a\rho_0 \cos \phi}} \right) \quad (4)$$

where  $z_1 = -\Delta/2 - z$  and  $z_2 = \Delta/2 - z$ . The upper signs in (4) are used when  $z_1, z_2 > 0$  and lower signs when  $z_1, z_2 < 0$  to reduce loss of precision. Eq. (4) must be integrated numerically over  $\phi$ , and when the evaluation point is on or near the segment with  $z_1 < 0 < z_2$  it involves a singularity or near singularity. However, it can be written as

$$K_z(\rho, z, \phi) = -\log(a^2 + \rho_0^2 - 2a\rho_0 \cos \phi) + \log \left[ \left( -z_1 + \sqrt{a^2 + z_1^2 + \rho_0^2 - 2a\rho_0 \cos \phi} \right) \left( z_2 + \sqrt{a^2 + z_2^2 + \rho_0^2 - 2a\rho_0 \cos \phi} \right) \right] \quad (5)$$

where the singularity is contained in the first term, which can be integrated in closed form as

$$\int_{-\pi}^{\pi} \log(a^2 + \rho_0^2 - 2a\rho_0 \cos \phi) d\phi = 4\pi \log[\max(a, \rho_0)].$$

The second term in (5) can be integrated with a low-order Gauss-Legendre rule, except when the evaluation point is near an end of the segment ( $z_1$  or  $z_2 \approx 0$ ) when a simple singularity extraction can be used.

The accuracy of the reduced and extended kernels were compared using numerical evaluation of the integrals in the program Mathematica<sup>TM</sup> (Wolfram Research). The NIntegrate function in Mathematica can numerically evaluate integrals including integrable singularities, so can be used to evaluate the integrals (1), (2) and (3) including when the evaluation point is on the wire surface.

The errors of the ETWK and RTWK over a range of segment lengths  $\Delta$  and radius  $a$  are shown in Fig. 1 for the self-term evaluation at the center of the segment. The ETWK was evaluated at the wire surface,  $K_1(a, 0)$ . The RTWK was evaluated at the center of the segment,  $K_0(0, 0)$ , since this is the way it is used, and it resulted in smaller errors relative to the exact kernel than evaluating on the surface at 90 degrees from the current filament. The error in the ETWK is seen to be nearly independent of  $\Delta$  and to increase with increasing radius  $a$  due to the approximate evaluation of the first integral in (2) containing the phase information. The error in the RTWK depends on the thickness ratio, and is poor when  $\Delta/a$  is on the order of 1 or less. For points off of the segment, with increasing  $\rho$  and  $z = 0$ , the error in the ETWK remains limited by phase error. For the RTWK the error related to  $\Delta/a$  decreases with increasing  $\rho$ , and phase becomes the dominant error. With  $\rho = a$  and increasing  $z$  relative to  $\max(\Delta, a)$  both the phase error and error related to  $\Delta/a$  decrease, with the ETWK remaining more accurate than the RTWK.

The RTWK and ETWK were compared by running NEC-4, a point matched EFIE code with RTWK and NEC-5, a mixed potential code with triangular and roof-top basis functions and input similar to NEC-4 that can use the RTWK or ETWK. Solutions for current on a dipole with length  $L = 0.5\lambda$  and radius  $a = 0.01\lambda$  (thickness parameter  $\Omega = 2 \log(L/a) = 7.8$ ) using the RTWK in NEC-5 are shown in Fig. 2. With 320 segments the current blows up to large values near the source and ends. Instability also occurs with 80 and 160 segments but is covered in the plot. Solutions obtained with the NEC-5 ETWK are plotted in Fig. 3 and show no instability up to 640 segments. The input admittance plotted in Fig. 4 demonstrates the stability of the ETWK with decreasing  $\Delta/a$ . The relatively large difference between NEC-4 and NEC-5 for large  $\Delta/a$  is due to NEC-4 converging considerably faster than NEC-5 with triangular basis functions near the  $\lambda/2$  resonance. Similar differences in stability are seen with a square loop model, where short segments are buried inside each other at the corners.

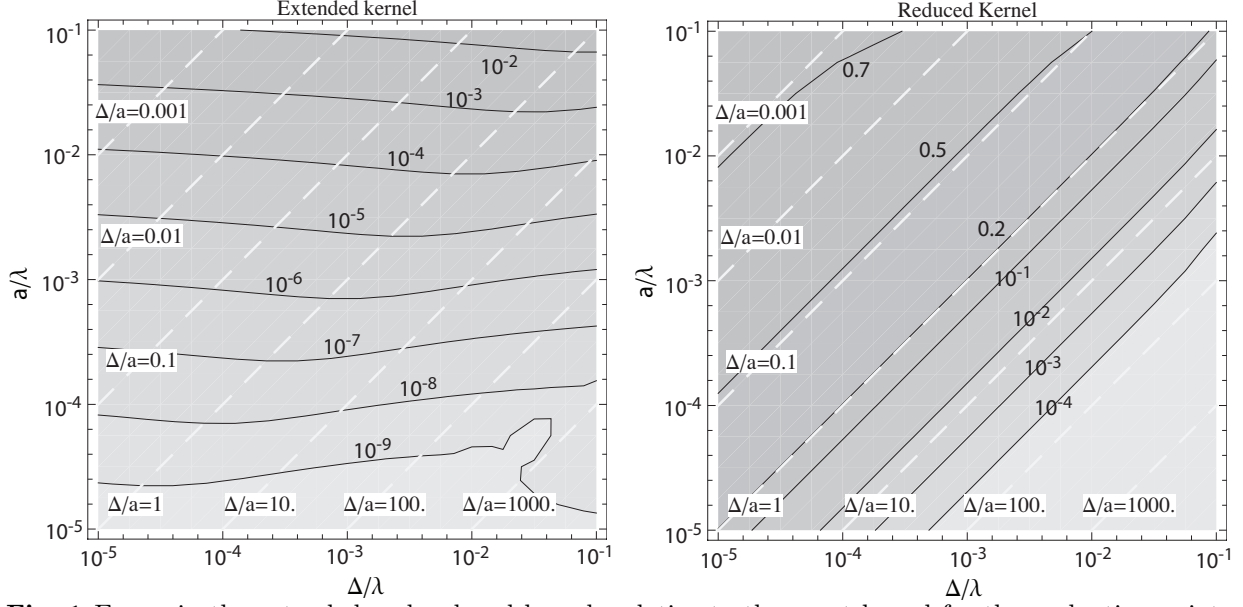


**Fig. 1** Errors in the extended and reduced kernels relative to the exact kernel for the evaluation point at the center of the segment (self-term) with  $\rho = a$  for the extended kernel,  $\rho = 0$  for the reduced kernel.

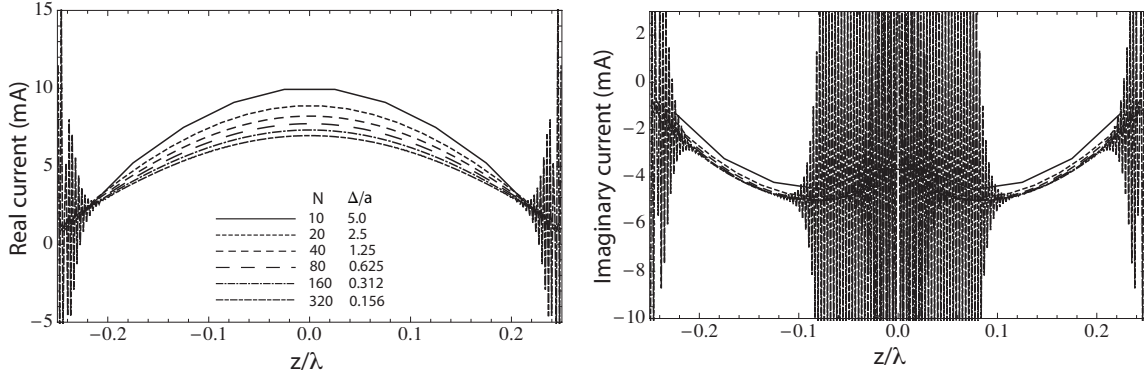


**Fig. 2** Current on a  $\lambda/2$  dipole with radius  $a = 0.01\lambda$  modeled with  $N$  segments using the RTWK in NEC-5.

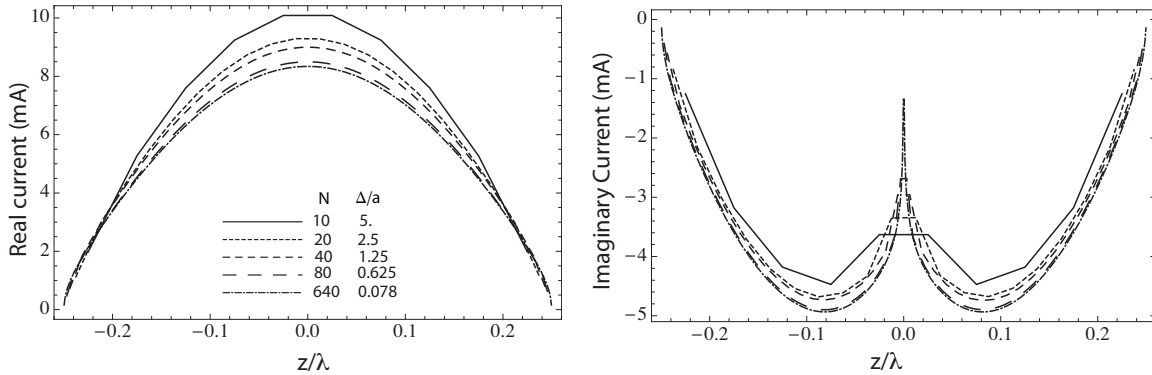


**Fig. 3** Current on a  $\lambda/2$  dipole with radius  $a = 0.01\lambda$  modeled with  $N$  segments using the ETWK in NEC-5.

Another model testing the wire kernel is a parallel-wire transmission line as the wires become close together. Transmission lines are often modeled with terminating wires for the source and loads, but that can mix wires close together and small  $\Delta/a$  at the ends. To avoid this problem a single  $10\lambda$  wire with radius  $a = 0.001\lambda$  was modeled over a PEC

ground with a voltage source at the center. This model can be cut in half to yield an end fed transmission line with open termination. Transmission line equations were used to get the effective characteristic impedance from the computed input impedance of the open line. Results are shown in Fig. 5. The RTWK and ETWK yield nearly identical results with only a patch model in closer agreement with the ideal  $Z_0$ . The patch model had 8 rectangular patches around the wire to allow the current to concentrate between the wires, which cannot happen in a thin-wire model.

The ETWK is seen to yield stable solutions with vary small  $\Delta/a$  as with the exact kernel, although there are reports of higher matrix condition number on large problems than with the exact kernel (Nathan Champagne, private communication).

### References

- [1] D. H. Werner, "An Exact Formulation for the Vector Potential of a Cylindrical Antenna with Uniformly Distributed Current and Arbitrary Radius," *IEEE Trans. Antennas and Propagation*, Vol. 41, No. 8, pp. 1009-1018, Aug. 1993.
- [2] D. H. Werner, "A Method of Moments Approach for the Efficient and Accurate Modeling of Moderately Thick Cylindrical Wire Antennas," *IEEE Trans. Antennas and Propagation*, Vol. 46, No. 3, pp. 373-381, March 1998.
- [3] D. R. Wilton and N. J. Champagne, "Evaluation and Integration of the Thin Wire Kernel," *IEEE Trans. Antennas and Propagation*, Vol. 54, No. 4, pp. 1200-1206, April 2006.
- [4] S. U. Hwu and D. R. Wilton, *Electromagnetic Scattering and Radiation by Arbitrary Configurations of Conducting Bodies and Wires*, Tech. Rept. 87-17, University of Houston, May 23, 1988.

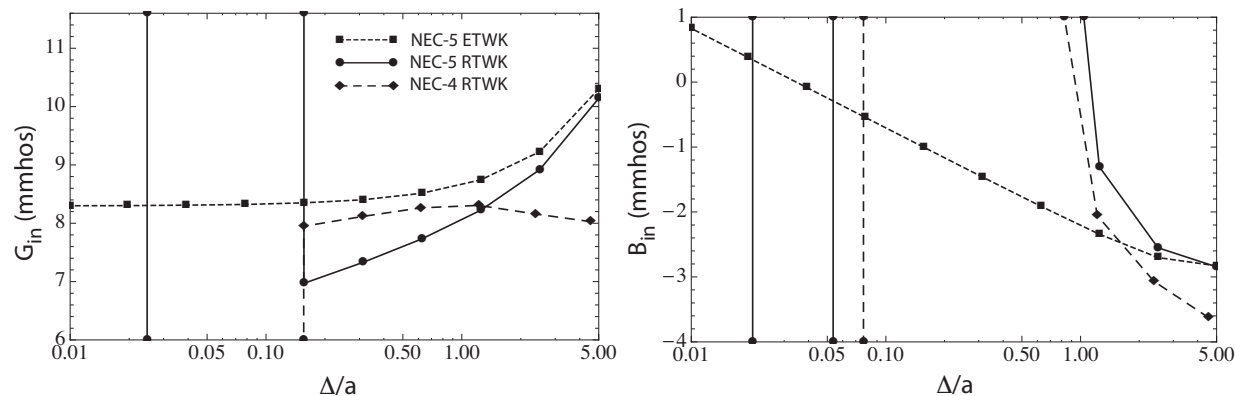


Fig. 4 Computed input admittance of a  $\lambda/2$  dipole with radius  $a = 0.01\lambda$  for varying segment length  $\Delta$ .

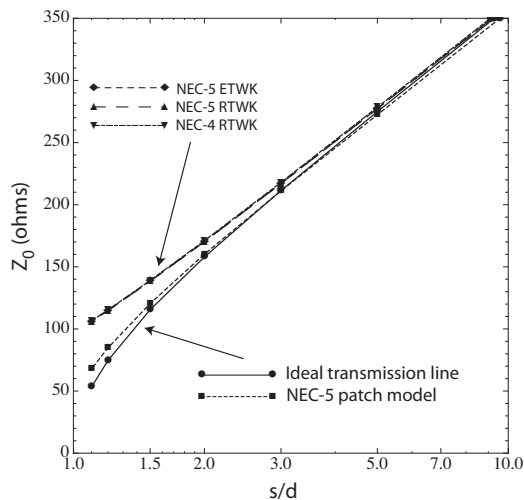


Fig. 5 Characteristic impedance of a two-wire transmission line with wire diameter  $d$  and separation  $s$  determined from numerical modeling.